

- [6] M. J. Bearpark, F. Bernardi, S. Clifford, M. Olivucci, M. A. Robb, B. R. Smith, T. Vreven, *J. Am. Chem. Soc.* **1996**, *118*, 169–175.
- [7] M. J. Bearpark, F. Bernardi, M. Olivucci, M. A. Robb, B. R. Smith, *J. Am. Chem. Soc.* **1996**, *118*, 5254–5260.
- [8] P. Celani, M. Garavelli, S. Ottani, F. Bernardi, M. A. Robb, M. Olivucci, *J. Am. Chem. Soc.* **1995**, *117*, 11584–11585.
- [9] L. Salem, *J. Am. Chem. Soc.* **1974**, *96*, 3486–3501.
- [10] W. M. Nau, *EPA Newsl.* **2000**, *70*, 6–29.
- [11] M. Klessinger, *Pure Appl. Chem.* **1997**, *69*, 773.
- [12] B. O. Roos, *Acc. Chem. Res.* **1999**, *32*, 137–144.
- [13] J. Finley, P.-Å. Malmqvist, B. O. Roos, L. Serrano-Andrés, *Chem. Phys. Lett.* **1998**, *288*, 299–306.
- [14] Geometry optimization and reaction path computations have been carried out at the CASSCF level of theory using a complete active space including twelve electrons in ten orbitals. The orbitals comprise the  $\pi$  and  $\pi^*$  N=N orbitals, the four  $\sigma$  and  $\sigma^*$  C–N orbitals, the two N lone-pair orbitals of the pyrazoline fragment, and the  $\sigma$  and  $\sigma^*$  orbitals of the reactive C–H bond of  $\text{CH}_2\text{Cl}_2$ . To improve the description of the H transfer, the standard 6-31G\* basis set (double- $\zeta$  plus d-type polarization functions on first- and second-row atoms) has been augmented with p-type polarization and s-type diffuse functions on the methylene chloride hydrogen atoms and with sp-type diffuse functions included in Gaussian98<sup>[15]</sup> on the nitrogen centers. Due to wavefunction instability, the  $S_0$  transition state (TS) has been optimized using state-average CASSCF with a  $S_0$  and  $S_1$  weight of 0.5. The relaxation coordinates have been computed according to the following procedure: a) The CI between the excited state ( $S_1$ ) and ground state ( $S_0$ ) was optimized using the methodology available in Gaussian98; b) the  $S_0$  relaxation paths were computed starting from the optimized CI point and using the IRD method described in references [16, 17]. The reaction path branches associated to the optimized TS were computed using the standard IRC method. In order to get a more accurate reaction energetics we re-evaluated the energy along a selected series of relaxation coordinate points using the multireference Møller–Plesset perturbation theory (CASPT2) using MOLCAS-4.<sup>[18]</sup> The  $S_1$  and  $S_0$  energies at CI and TS, where the energy gap is small, were re-evaluated using the MS-CASPT2 procedure.<sup>[13]</sup>
- [15] *Gaussian98 (Revision A.7)*, M. J. Frisch, G. W. Trucks, H. B. Schlegel, G. E. Scuseria, M. A. Robb, J. R. Cheeseman, V. G. Zakrzewski, J. A. Montgomery, R. E. Stratmann, J. C. Burant, S. Dapprich, J. M. Millam, A. D. Daniels, K. N. Kudin, M. C. Strain, O. Farkas, J. Tomasi, V. Barone, M. Cossi, R. Cammi, B. Mennucci, C. Pomelli, C. Adamo, S. Clifford, J. Ochterski, G. A. Petersson, P. Y. Ayala, Q. Cui, K. Morokuma, D. K. Malick, A. D. Rabuck, K. Raghavachari, J. B. Foresman, J. Cioslowski, J. V. Ortiz, A. G. Baboul, B. B. Stefanov, G. Liu, A. Liashenko, P. Piskorz, I. Komaromi, R. Gomperts, R. L. Martin, D. J. Fox, T. Keith, M. A. Al-Laham, C. Y. Peng, A. Nanayakkara, C. Gonzalez, M. Challacombe, P. M. W. Gill, B. G. Johnson, W. Chen, M. W. Wong, J. L. Andres, M. Head-Gordon, E. S. Replogle, J. A. Pople, Gaussian, Inc., Pittsburgh, PA, **1998**.
- [16] P. Celani, M. A. Robb, M. Garavelli, F. Bernardi, M. Olivucci, *Chem. Phys. Lett.* **1995**, *243*, 1–8.
- [17] M. Garavelli, P. Celani, M. Fato, M. J. Bearpark, B. R. Smith, M. Olivucci, M. A. Robb, *J. Phys. Chem.* **1997**, *101*, 2023–2032.
- [18] *MOLCAS, Version 4*, K. Andersson, M. R. A. Blomberg, M. P. Fülscher, G. Karlström, R. Lundh, P.-Å. Malmqvist, P. Neogrády, J. Olsen, B. O. Roos, A. J. Sadlej, M. Schütz, L. Seijo, L. Serrano-Andrés, P. E. M. Siegbahn, P.-O. Widmark, University of Lund, Lund, Sweden **1997**.
- [19] J. Saltiel, P. T. Shannon, O. C. Zafiriou, A. K. Uriarte, *J. Am. Chem. Soc.* **1980**, *102*, 6799–6808.
- [20] R. D. Levine, R. B. Bernstein, *Molecular Reaction Dynamics and Chemical Reactivity*, Oxford University Press, New York, NY, **1987**.
- [21] M. Polanyi, *Atomic Reaction*, Williams and Norgate, London, **1932**.
- [22] The photolysis experiments were carried out using a 900 W xenon source and high radiance monochromator (Applied Photophysics Ltd) at  $\lambda = 380$  nm. For the EPR experiments, fresh chloroform solutions with the spin trap PBN (3 mm) and DBO (6 mm) were thoroughly deaerated with oxygen-free nitrogen for at least 20 min. EPR spectra were recorded at room temperature on a Bruker 200D SRC instrument equipped with a microwave frequency counter XL (Jagmar). The spectrometer was interfaced with a PS/2 technical instrument hardware computer and the data acquired using the EPR data system CS-EPR (Stelar Inc.). Simulations of the EPR spectra were performed using a home-made program. The irradiation in the absence of DBO led to no detectable signal.
- [23] Spin Trap Data Base, NIEHS (National Institute of Environmental Health Sciences) **2001**.
- [24] The formation of protonated DBO upon photolysis of DBO in chloroform was also observed by Feth and Greiner (University of Stuttgart-Hohenheim). We are grateful for this information and related fruitful discussions.
- [25] J. R. Pliego, Jr., W. B. De Almeida, *J. Phys. Chem.* **1996**, *100*, 12410–12413.
- [26] L. Blancafort, F. Jolibois, M. Olivucci, M. A. Robb, *J. Am. Chem. Soc.* **2001**, *123*, 722–732.
- [27] E. Fernández, L. Blancafort, M. Olivucci, M. A. Robb, *J. Am. Chem. Soc.* **2000**, *122*, 7528–7533.
- [28] M. Garavelli, C. S. Page, P. Celani, M. Olivucci, W. E. Schmid, S. A. Trushin, W. Fuss, *J. Phys. Chem. A* **2001**, *105*, 4458–4469.

## Molecular Recognition of UDP-Gal by $\beta$ -1,4-Galactosyltransferase T1\*\*

Thorsten Biet and Thomas Peters\*

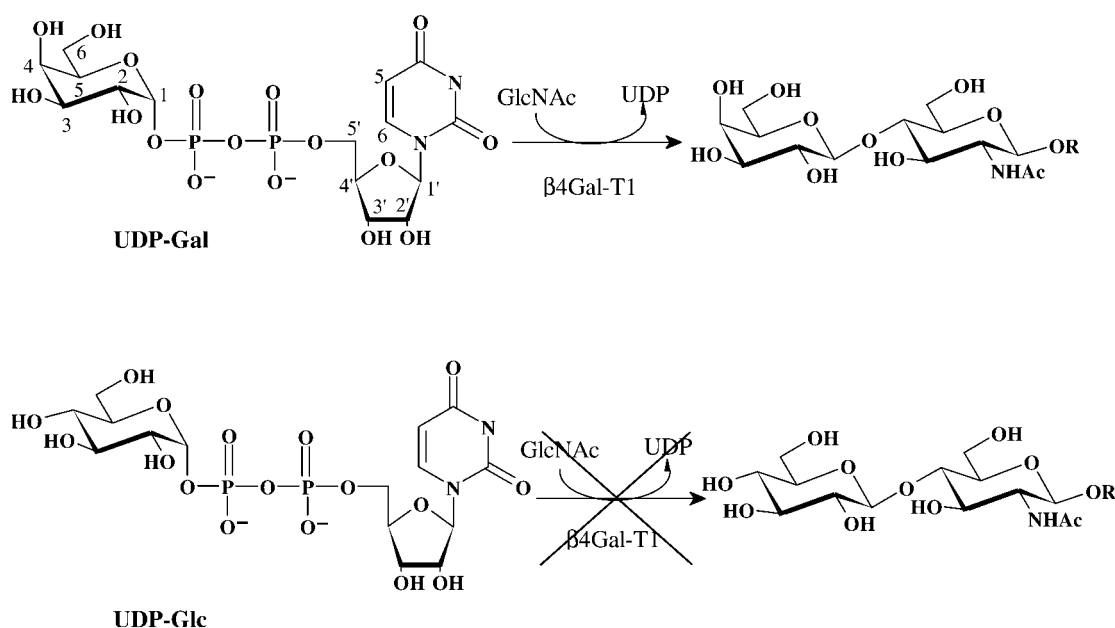
Dedicated to Professor Joachim Thiem  
on the occasion of his 60th birthday

In mammals, protein–carbohydrate interactions play a crucial role in mediating a variety of biological recognition processes.<sup>[1]</sup> The enzymes responsible for the biosynthesis of glycan chains are glycosyltransferases, and their malfunction leads to a number of pathological disorders. So far, only limited data are available for the three-dimensional structure of mammalian glycosyltransferases.<sup>[2]</sup> Recently, an X-ray structure was published of  $\beta$ -1,4-galactosyl-transferase ( $\beta$ 4Gal-T1, EC 2.4.1.90/38), a Golgi-resident membrane-bound enzyme, in its free and substrate-bound form.<sup>[2c]</sup> This transferase is responsible for the transfer of galactose from UDP-Gal (uridine diphospho-D-galactose, Scheme 1) to  $\beta$ -D-N-acetylglucosamine residues, furnishing poly-N-acetylglucosamine chains found in glycoproteins and glycosphingolipids. The enzyme  $\beta$ 4Gal-T1 cocrystallized with the donor substrate UDP-Gal, but the electron density was not sufficient to resolve the terminal galactose residue. Therefore, crucial molecular details of the recognition reaction between  $\beta$ 4Gal-

[\*] Prof. Dr. T. Peters, Dipl.-Chem. T. Biet  
Institut für Chemie, Medizinische Universität zu Lübeck  
Ratzeburger Allee 160, 23538 Lübeck (Germany)  
Fax: (+49) 451-500-4241  
E-mail: thomas.peters@chemie.mu-luebeck.de

[\*\*] This work was supported by the BMBF (FKZ 031161) and the DFG (Teilprojekt B3 of SFB 470). Financial support from the Verband der Chemischen Industrie is gratefully acknowledged. Dr. T. Keller and Dr. G. Wolff (Bruker Analytik GmbH, Rheinstetten) are thanked for excellent support.

Supporting information for this article is available on the WWW under <http://www.angewandte.com> or from the author.



Scheme 1.  $\beta 4\text{Gal-T1}$  transfers D-Galactose from UDP-Gal to D-GlcNAc residues (top reaction). The enzyme is highly specific; for example, it does not process UDP-Glc (bottom reaction) at a significant rate.<sup>[8]</sup>

T1 and UDP-Gal still must to be revealed. Here we present NMR data that map the binding epitope of UDP-Gal bound to  $\beta 4\text{Gal-T1}$  with atomic resolution.

Several NMR experiments are now known for the analysis of protein–ligand interactions. Recently, saturation transfer difference (STD) spectroscopy was introduced for the screening of compound libraries for binding activity towards receptor proteins.<sup>[3]</sup> The method has proven to be very robust, and requires only small amounts of protein in the  $\mu\text{M}$  range.<sup>[4]</sup> The STD NMR technique is also very useful to map the binding epitope of ligands with atomic resolution.<sup>[5]</sup> Ligand protons that are in close contact with the protein binding pocket experience a larger fraction of saturation transfer than protons further away. Therefore, protons belonging to the binding epitope of the ligand show larger signal intensities than other ligand protons in the STD NMR spectra. This in turn allows precise definition of the binding epitope.

To study the binding of UDP-Gal to  $\beta 4\text{Gal-T1}$ <sup>[6]</sup> we prepared an NMR sample that contained about a 45-fold molar excess of UDP-Gal over  $\beta 4\text{Gal-T1}$ . To avoid complications from paramagnetic  $\text{Mn}^{2+}$  we substituted  $\text{Mn}^{2+}$  by  $\text{Mg}^{2+}$  in the buffer. This is known to reduce the activity of the enzyme but its functionality is retained.<sup>[7]</sup> One-dimensional STD NMR spectra were obtained for this sample with saturation times ranging from 0.5–2.0 s. Figure 1b shows the STD spectrum with 2.0 s saturation time; for comparison the 1D  $^1\text{H}$  NMR spectrum of UDP-Gal is shown in Figure 1a.

From the STD spectra the relative amount of saturation transfer for each individual proton was calculated utilizing a corresponding 1D NMR spectrum as reference (Scheme 2).<sup>[5]</sup> These values reflect the degree of dipolar interactions of UDP-Gal protons with protons belonging to the active site of the enzyme.

It is clear that the ribose and uracil protons receive the largest amount of saturation transfer. From the ribose residue, the anomeric proton H1' and the proton H4' give the most

intense STD responses. This is in accordance with the X-ray structure, where the uridine is located in a pronounced binding pocket. Uracil displays a stacking interaction with Phe226, and as a result H1' and H4' of the ribose point towards the interior of the protein, which explains their prominent STD signals. The galactose residue shows smaller STD effects, indicating that this residue is in less intimate contact with the protein surface. Since the galactose residue has to be transferred to an acceptor substrate during the enzymatic reaction, it is reasonable that its contact with the protein's active site is not too tight.

All the protons of the galactose residue show a response in the STD spectrum, indicating that galactose is in direct contact with the enzyme binding pocket. From the galactose protons, H4 and H2 lead to the most prominent STD signals. For comparison, the binding of UDP-Glc (uridine diphosphate-D-glucose) to  $\beta 4\text{Gal-T1}$  was studied. For UDP-Glc in the presence of  $\beta 4\text{Gal-T1}$ , STD spectra were obtained also; therefore, binding still occurs. In general, all STD effects were considerably smaller than for UDP-Gal, indicating a much smaller binding affinity (Figure 1). STD effects were only observed for the ribose unit and for uracil; there were no STD responses for the glucose residue. It may be argued that H1 of glucose receives small amounts of saturation, but it was impossible to quantify this effect (Figure 1d). It is concluded that glucose is not in direct contact with the enzyme active site. Apparently, the enzyme does not recognize the glucose residue, and therefore probably fails to properly align the monosaccharide moiety for the transfer. This explains the observation that  $\beta 4\text{Gal-T1}$  does not transfer glucose residues at a significant rate.<sup>[8]</sup> The finding is also in agreement with the X-ray structure of  $\beta 4\text{Gal-T1}$  complexed with uridine diphosphogalactose. An inspection of the orientation of UDP in the binding pocket of  $\beta 4\text{Gal-T1}$  shows that a monosaccharide attached to the terminal phosphate of UDP may have a variety of orientations. Therefore, specific interactions with

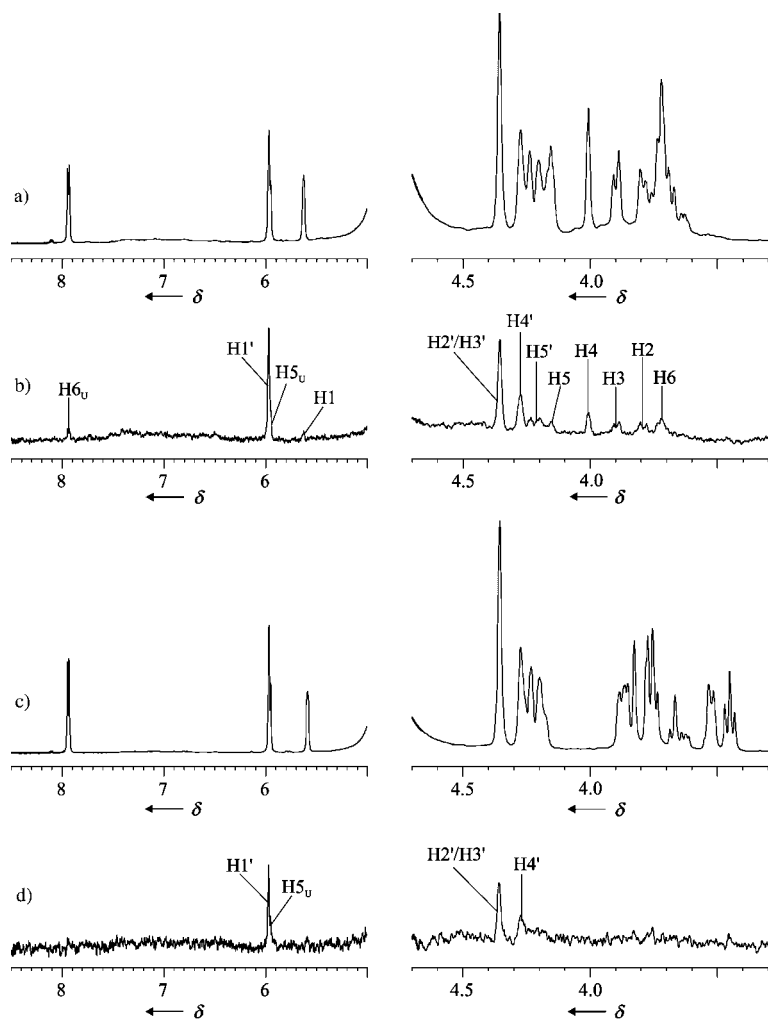
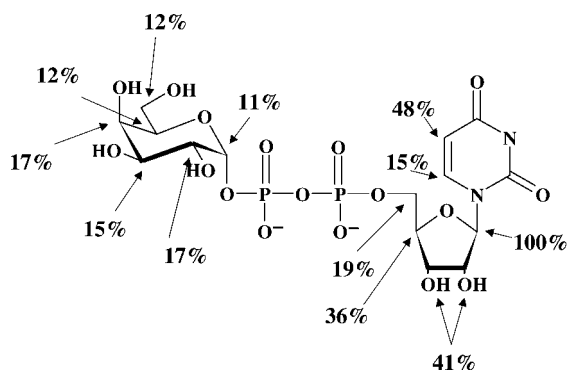


Figure 1. One-dimensional STD NMR (500 MHz) spectra for UDP-Gal (b, 16-fold amplification) and UDP-Glc (d, 32-fold amplification) in the presence of  $\beta$ 4Gal-T1 as well as the corresponding  $^1\text{H}$  NMR reference spectra for free UDP-Gal (a) and UDP-Glc (c). The STD spectra were acquired with selective presaturation at  $\delta=0$  for a duration of 2 s utilizing a cascade of gaussian pulses (duration 50 ms, spacing 1 ms). 2 k scans were recorded for the STD spectra, and 1 K scans for the reference  $^1\text{H}$  NMR spectra. From the spectra relative STD effects were determined (see Scheme 2).



Scheme 2. Relative STD effects for UDP-Gal bound to  $\beta$ 4Gal-T1. The values were calculated by determining the individual signal intensities in the STD spectrum ( $I_{\text{STD}}$ ) and in the reference 1D NMR spectrum ( $I_0$ ).<sup>[5]</sup> The ratios of the intensities  $I_{\text{STD}}/I_0$  were normalized using the largest STD effect (anomeric proton H1' of the ribose unit, 100%) as a reference. The arrows indicate the position of the proton experiencing an STD effect. The value of 41% corresponds to the cumulative saturation transfer for H2' and H3'. Likewise, 12% denotes the sum effect for both protons H6 of the galactose residue. The values for protons H5 and H5' are estimates only because separate integration of the two signals was difficult.

amino acids will be required to establish binding interactions. We propose that the glucose residue of UDP-Glc protrudes from the binding site, whereas the galactose residue of UDP-Gal is in intimate contact with binding-site protons, as this is reflected by the STD NMR experiments.

The fact that the UDP part of UDP-Glc is bound to the protein is reasonable, as it is known that UMP and UDP as well as their derivatives—for example, UDP-Fuc (uridine diphospho-L-fucose) and UDP-Man (uridine diphospho-D-mannose)—inhibit  $\beta$ 4Gal-T1.<sup>[9a]</sup> The results are consistent with several previous studies where a variety of UDP-Gal derivatives had been synthesized to determine the relative rates of transfer of galactose from UDP-Gal to *N*-acetylglucosamine.<sup>[8, 9]</sup> It was found that any variation of the galactose moiety reduced the transfer rate. Deoxygenation of the 2-position of galactose only had a minor influence,<sup>[9c]</sup> but sterically demanding substituents in this position significantly reduced the transfer rate.<sup>[8a]</sup> The most pronounced effect was observed upon modifying the 4- and the 2-position of galactose in concert; for example, for UDP-GlcNAc (uridine diphospho-*N*-acetyl-D-glucosamine) as a donor substrate no transfer activity was observed. Modification of these two positions lead to almost inactive donor substrates.<sup>[8a]</sup> This corresponds well with the finding that protons H4 and H2 of galactose receive the largest fraction of saturation transfer (Scheme 2).

Control experiments were performed with UDP-Gal in the presence of two lectins, *Aleuria aurantia* agglutinin (AAA) and *Sambucus nigra* agglutinin (SNA), to exclude the possibility that the effects observed were nonspecific (see the Supporting Information). Lectin AAA specifically recognizes L-fucose moieties,<sup>[10]</sup> whereas SNA binds to D-galactose, and most tightly to epitopes containing the disaccharide  $\alpha$ -D-Neu5Ac-(2,3)-D-Gal.<sup>[4b, 11]</sup> In the presence of AAA, UDP-Gal showed no STD effects. L-Fucose, which was also present in the same sample, clearly displayed STD signals. In the presence of SNA, UDP-Gal showed strong STD effects for the galactose moiety, and rather weak effects for the rest of the molecule. Thus, individual STD signal patterns were observed upon addition of UDP-Gal for each of the three different proteins,  $\beta$ 4Gal-T1, AAA, and SNA, demonstrating that the STD spectra reflect the binding epitope in each case.

Our NMR experiments show that  $\beta$ 4Gal-T1 binds to UDP-Gal and to UDP-Glc, albeit with a lower affinity to the latter. Whereas in the case of UDP-Glc only the UDP part of the ligand is in contact with the protein surface, the complete UDP-Gal molecule binds to  $\beta$ 4Gal-T1. A quantitative analysis of STD effects allowed definition of the binding epitope of UDP-Gal with atomic resolution. With this technique it will be possible to study the binding of substrates to a variety of glycosyltransferases. Therefore, we are currently applying the method to screen other mammalian glycosyltransferases for which no X-ray data are yet available. The information about

the binding epitopes will be of crucial importance for the design of new selective and potent glycosyltransferase inhibitors.

## Experimental Section

All spectra were acquired on a Bruker DRX 500MHz spectrometer with a 5-mm TXI probehead. The STD spectra were measured at 293 K with 2 k scans. The reference spectra were measured with 1 k scans. Saturation transfer was achieved by using 40 selective gaussian pulses (duration 50 ms, spacing 1 ms). The protein envelope was irradiated at  $\delta = 0$  (on-resonance) and  $\delta = 40$  (off-resonance). Subsequent subtraction was achieved by phase cycling.

The concentrations of  $\beta$ 4Gal-T1 were 20  $\mu$ M and 7  $\mu$ M for UDP-Gal and UDP-Glc, respectively. Sample volume: 300  $\mu$ L in a Shigemi tube. The concentration of UDP-Gal was 0.9 mM (UDP-Glc 1 mM). Buffer: 20 mM Tris, 20 mM NaCl, 10 mM MgCl<sub>2</sub> pH 7.4 (not corrected).

Received: May 14, 2001 [Z17095]

- [1] For an overview, see A. Varki, R. Cummings, J. Esko, H. Freeze, G. Hart, J. Marth, *Essentials of Glycobiology*, Cold Spring Harbor Laboratory Press, Cold Spring Harbor, New York, **1999**.
- [2] a) L. N. Gastinel, C. Bignon, A. K. Misra, O. Hindsgaul, J. H. Shaper, D. H. Joziasse, *EMBO J.* **2001**, *20*, 638–649; b) U. M. Unligil, S. Zhou, S. Yuwaraj, M. Sarkar, H. Schachter, J. M. Rini, *EMBO J.* **2000**, *19*, 5269–5280; c) L. N. Gastinel, C. Cambillau, Y. Bourne, *EMBO J.* **1999**, *18*, 3546–3557; d) U. M. Unligil, J. M. Rini, *Curr. Opin. Struct. Biol.* **2000**, *10*, 510–517.
- [3] M. Mayer, B. Meyer, *Angew. Chem.* **1999**, *111*, 1902–1906; *Angew. Chem. Int. Ed.* **1999**, *38*, 1784–1788.
- [4] a) J. Klein, R. Meinecke, M. Mayer, B. Meyer, *J. Am. Chem. Soc.* **1999**, *121*, 5336–5337; b) M. Vogtherr, T. Peters, *J. Am. Chem. Soc.* **2000**, *122*, 6093–6099; c) H. Maaheimo, P. Kosma, L. Brade, H. Brade, T. Peters, *Biochemistry* **2000**, *39*, 12778–12788.
- [5] M. Mayer, B. Meyer, *J. Am. Chem. Soc.* **2001**, *123*, 6108–6117.
- [6] Recombinant bovine  $\beta$ 4Gal-T1 ( $M_w$  38 kDa) and synthetic UDP-Gal ( $M_w$  610.3 Da) were purchased from Calbiochem.
- [7] N. J. Kuhn, S. Ward, W. S. Leong, *Eur. J. Biochem.* **1991**, *195*, 243–250.
- [8] a) M. M. Palcic, O. Hindsgaul, *Glycobiology* **1991**, *1*, 205–209; b) L. J. Berliner, R. D. Robinson, *Biochemistry* **1982**, *21*, 6340–6343.
- [9] a) T. Endo, Y. Kajihara, H. Kodama, H. Hashimoto, *Bioorg. Med. Chem.* **1996**, *4*, 1939–1948; b) Y. Kajihara, T. Endo, H. Ogasawara, H. Kodama, H. Hashimoto, *Carbohydr. Res.* **1995**, *269*, 273–294; c) G. Srivastava, O. Hindsgaul, M. M. Palcic, *Carbohydr. Res.* **1993**, *245*, 137–144; d) H. Yuasa, O. Hindsgaul, M. M. Palcic, *J. Am. Chem. Soc.* **1992**, *114*, 5891–5892.
- [10] a) H. Debray, J. Montreuil, *Carbohydr. Res.* **1989**, *185*, 15–26; b) F. Fukumori, N. Takeuchi, T. Hagiwara, H. Ohbayashi, T. Endo, N. Kochibe, Y. Nagata, A. Kobata, *J. Biochem.* **1990**, *107*, 190–196; c) T. Weimar, T. Peters, *Angew. Chem.* **1994**, *106*, 79–82; *Angew. Chem. Int. Ed.* **1994**, *33*, 88–91.
- [11] a) W. F. Broekaert, M. Nsimba-Lubaki, B. Peeters, W. J. Peumans, *Biochem. J.* **1984**, *221*, 163–169; b) E. J. M. Van Damme, A. Barre, P. Rougé, F. Van Leuven, W. J. Peumans, *Eur. J. Biochem.* **1996**, *235*, 128–137.

## Watching the Photo-Oxidation of a Single Aromatic Hydrocarbon Molecule\*\*

Thomas Christ, Florian Kulzer, Patrice Bordat, and Thomas Basché\*

The ability to observe chemical reactions at the level of single molecules has been demonstrated by fluorescence microscopy.<sup>[1]</sup> Actually, every optical single-molecule experiment with organic fluorophores under ambient conditions is eventually terminated by a photochemical reaction, which converts the molecule into a state in which it no longer absorbs or fluoresces. Often this photobleaching of organic fluorophores depends on the presence of oxygen, the influence of which on the photophysics and -chemistry of the fluorophores has been elucidated in recent single-molecule experiments.<sup>[2]</sup> Although photobleaching quite generally is an important mechanism for the degradation of organic dye molecules under ambient conditions, understanding of this process is limited especially for the class of comparatively photo-stable dyes used in single-molecule spectroscopy or for technological applications. For single terrylene molecules in a *p*-terphenyl host crystal, we can unambiguously show that a self-sensitized photo-oxidation is the initial step or directly leads to the terminal photobleaching.

The fluorescence of single terrylene molecules in a *p*-terphenyl host crystal<sup>[3]</sup> was imaged by confocal microscopy. When following the fluorescence intensity as a function of time (emission time trace) under ambient conditions, various types of intensity changes are observed. Either the fluorescence signal drops to the background level irreversibly after a period of constant emission intensity (Figure 1a) or it jumps to a new level after having dropped to the background level for a short period of time (Figure 1c). As seen in Figure 1c, the latter sequence of events in this case is also terminated by an irreversible drop of the fluorescence signal to the background level. In addition to the time traces, a complete sequence of emission spectra of the molecules under study is recorded simultaneously at regular intervals (5 s). For the molecule, the time trace of which is shown in Figure 1a, all emission spectra are identical until the emission ceases and fully agree with an ensemble spectrum of terrylene in *p*-terphenyl. The spectra in Figure 1d, which belong to the time trace in Figure 1c, shows however that after this molecule resumes emission at  $\sim 53$  s the spectrum has shifted by 40 nm to the blue. We attribute all the intensity and spectral changes to a photo-oxidation of terrylene or subsequent internal rearrangements of the primary photoproducts.

[\*] Prof. Dr. T. Basché, Dipl.-Chem. T. Christ, Dr. F. Kulzer  
Institut für Physikalische Chemie  
Johannes Gutenberg Universität Mainz, 55099 Mainz (Germany)  
Fax: (+49) 6131-3923953  
E-mail: thomas.basche@uni-mainz.de  
Dr. P. Bordat  
Max-Planck-Institut für Polymerforschung  
55128 Mainz (Germany)

[\*\*] This work was supported by the Fonds der Chemischen Industrie. We would like to thank R. Schmidt, M. Gudipati, and K. Müllen for very insightful discussions.